CMS CR -2011/341

The Compact Muon Solenoid Experiment

Conference Report

Mailing address: CMS CERN, CH-1211 GENEVA 23, Switzerland

01 December 2011 (v2, 03 December 2011)

Search for a Higgs boson decaying into two photons in the CMS detector

Roberta Volpe for the CMS Collaboration

Abstract

A search for a Higgs boson decaying into diphotons in pp collisions at the LHC at a center-of-mass energy of 7 TeV is presented. The analysis is performed on a dataset corresponding to 1.66 fb^{-1} of data recorded in 2011 by the CMS experiment. Limits are set on the cross section of a Standard Model Higgs boson decaying to two photons, and on the cross section of a fermiophobic Higgs boson decaying to two photons

Presented at *Lepton Photon 2011: XXV International Symposium on Lepton Photon Interactions at High Energies*

PRAMANA — journal of physics
© Indian Academy of Sciences
Vol. xx, No. x
xxxx xxxx
pp. 1–3

Search for a Higgs boson decaying into two photons in the CMS detector

ROBERTA VOLPE (ON BEHALF OF CMS COLLABORATION)[a, *]
[a]National Central University, Chung-Li, Taiwan

Abstract. A search for a Higgs boson decaying into two photons in pp collisions at the LHC at a center-of-mass energy of 7 TeV is presented. The analysis is performed on a dataset corresponding to 1.66 fb^{-1} of data recorded in 2011 by the CMS experiment. Limits are set on the cross section of a Standard Model Higgs boson decaying to two photons, and on the cross section of a fermiophobic Higgs boson decaying to two photons.

Keywords. CMS, LHC, Low mass Higgs, Photons, Electromagnetic Calorimeter

PACS Nos. 14.80.Cp,14.80.-j,12.60.-i

1. Motivation

$H \to \gamma\gamma$ is one of the most promising channels for Higgs discovery in the very low mass region. Despite its small branching ratio of about 0.2% in this region of interest, the $H \to \gamma\gamma$ decay channel provides a clean final-state topology, since the invariant mass of the two photons can be reconstructed with great precision and good resolution. This is possible thanks to the very good performances and the high granularity of the lead-tungstate crystal electromagnetic calorimeter (ECAL in the following) part of the CMS experiment detector [1]. The ECAL is constituted by a barrel (EB) covering the region $|\eta|$ [1]. < 1.442 and two endcaps (EE) which close the barrel, covering $1.556 < |\eta| < 2.5$. Calibration of the ECAL uses detailed inter-calibration of barrel supermodules and the changes in transparency of the crystals during LHC fills are monitored continuously. Also other CMS subsystems are used in the photon identification: the hadronic calorimeter (HCAL) and the tracker system. Besides the SM Higgs, the so called *fermiophobic* models (where Higgs boson only couples to bosons, for example [2] and references therein) has been searched for as well; in such a model the branching fraction to a photon pair is modified and, for a very low mass Higgs, greatly enhanced. The main features of the analysis are reported in the following, more details can be found in [3].

---

[*] `roberta.volpe@cern.ch`

[1] where the pseudorapidity η is defined as $\eta = -ln[tan(\theta/2)]$, with θ being the polar angle of the trajectory of the particle with respect to the counterclockwise beam direction

2. Diphoton pair selection

The analyzed events are collected by requiring two photons with very loose identification criteria at high level trigger step. The efficiency of such a requirement is almost 100%. The occurrence of multiple collisions (whose mean value is 6.5) in the same bunch crossing, pile up, affects the determination of the diphoton production vertex After a loose selection of two photons, two methods are used for the determination of the vertex: (i) use of kinematic properties of tracks associated to the vertex, in relation with the di-photon system; (ii) if there is a photon conversion track reconstructed, the closest reconstructed vertex to the point where the track points is chosen. By using the combination of these two methods, the probability to find Higgs boson vertices within 10 mm from their true location depends on $p_T(H)$, and, for $p_T(H) > 60$ GeV/c, is larger than 95%. The so-called R9 variable, that describes the compactness of the energy deposition in the ECAL, allows for discriminating converted and unconverted photons. Background from misidentified jets is more abundant in low than high R_9 and in EE than EB photons. Therefore, it is useful to define four event classes: both photons in EB and high R_9 (c_1); both photons in EB and at least one with low R_9 (c_2); at least a photon in EE and both with high R_9 (c_3); at least a photon in EE and at least one with low R_9 (c_4). The variables used in the photon identification are mainly cluster shape and isolation variables The threshold used for these variables are chosen by an iterative procedure in which each variable is checked after all the other cuts are applied. An S/B target value is chosen to be the same for every category.

The event selection requires two identified photons in the region covered by the EB or EE, with p_T >30 GeV/c and at least one with $p_T > 40$ CeV/c. The distribution of the di-photon invariant mass after the event selection is displayed in Fig. 1, where data are compared to the Monte Carlo (MC) processes, whose cross sections have been corrected with the k-factors derived from CMS 2010 data. The observed spectrum agrees with the distribution of MC simulation of SM processes within the MC cross section uncertainties (15%).

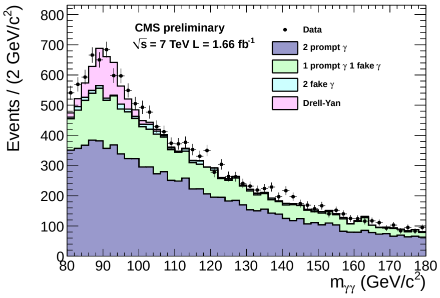

Figure 1.: Comparison between data and simulation of the di-photon invariant mass distribution.

3. Signal and Background modeling

The p_T of the di-photon system is used to further divide the four event classes, the p_T threshold is chosen to be $p_T(\gamma\gamma)$ = 40 GeV/c. It is useful for fermiophobic Higgs, since the associated production gives a boost to the di-photon system. Therefore, eight event classes have been separately analyzed to improve the statistical significance. The energy scale of ECAL has been inferred by using $Z \to e^+e^-$ events and correction factors are applied on photon candidates in data and simulation. A worsening of the photon energy resolution is needed for MC in order to reproduce the data resolution, such resolution gives an invariant mass resolution ranging from $\sigma_{eff} = 1.41$ GeV/c^2, for the best resolution event class (c_1 with $p_T(\gamma\gamma) >$ 40GeV/c), to $\sigma_{eff} = 3.59$ GeV/c^2 for the class c_4 with $p_T(\gamma\gamma) <$ 40GeV/c. The electron veto efficiency has been estimated by using a high-purity photon sample from $Z \to \mu\mu\gamma$ events. The efficiency of the other photon identification requirements was measured in data using $Z \to e^+e^-$ events and correcting for possible differences between electron and photon. MC is re-weighted to take into account the data/MC discrepancies ($< 1\%$) in the selection efficiency, vertex finding efficiency and the different pile up conditions with which the signal samples have been generated with respect to estimated PU in data. The background description is obtained by fitting the observed diphoton mass distributions in the eight event classes with 2^{nd} order Bernstein polynomials over the range $100 < m(\gamma\gamma) < 160$GeV/c^2.

4. Limit setting

The di-photon invariant mass distributions in each of the eight classes are considered separately and the combination of the results is used to set the upper limit at 95% C.L. Two methods have been compared: Modified frequentist method CL_S [4] with Profile Likelihood as test statistics and the Bayesian approach with a flat prior for the signal strength. Both binned and unbinned analises have been performed as cross check, and fine steps in the $m(\gamma\gamma)$ (500 MeV/c^2) are used to exploit the good resolution of the di-photon invariant mass. A detailed study was performed to estimate the systematic uncertainties. The main sources are the theoretical modeling of the cross-section of the gluon fusion production, the integrated luminosity, the class migration and the photon identification efficiency. The expected (observed) limit is between 2.7 and 4.7 (1.3 and 8) times the SM cross section. The observed limit at m($\gamma\gamma$) around 140 GeV has been measured to exceed the 2σ of the expected one with the local p-value of $(2.5 \pm 0.3) \cdot 10^{-3}$. The corresponding expected significance of this excess using look-else-where effect [5], is 1.6 σ and the most probable signal strength is $(4.5^{+1.7}_{-1.9}) \cdot \sigma_{SM}$. The upper limit set to the fermiophobic models is displayed in Fig. 2. fermiophobic Higgs is expected to be excluded in the mass range 110-116.5 GeV/c^2 and it has been observed an exclusion in the mass range 110-112 GeV/c^2 .

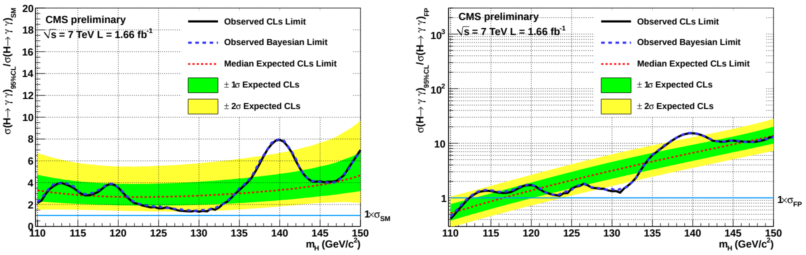

Figure 2.: Expected and observed upper limit to the ratio $\frac{\sigma}{\sigma_{model}}$ for the SM (left) and fermiophobic model (right).

References

[1] The CMS Collaboration, *JINST* **03 S08004** (2008). Doi:10.1088/1748-0221/3/08/S08004.
[2] S. Mrenna and J. D. Wells, *Phys. Rev. D 63, 015006 (2001)* **D63**, 015006 (2011).
[3] The CMS Collaboration, *CMS PAS HIG-11-021* (2011).
[4] A. L. Read, *J. Phys. G: Nucl. Part. Phys.* **28**, 2693 (2002).
[5] Ofer Vitells Eilam Gross, *Eur.Phys.J.* **C70**, 525 (2010).